Q-REAL: Towards Realism and Plausibility Evaluation for AI-Generated Content

Shushi Wang¹ Zicheng Zhang³ Chunyi Li¹ Wei Wang² Liya Ma² Fengjiao Chen² Xiaoyu Li² Xuezhi Cao² Guangtao Zhai¹ Xiaohong Liu^{1,4†}

¹Shanghai Jiao Tong University ²Meituan ³Shanghai AI Lab ⁴Shanghai Innovation Institute

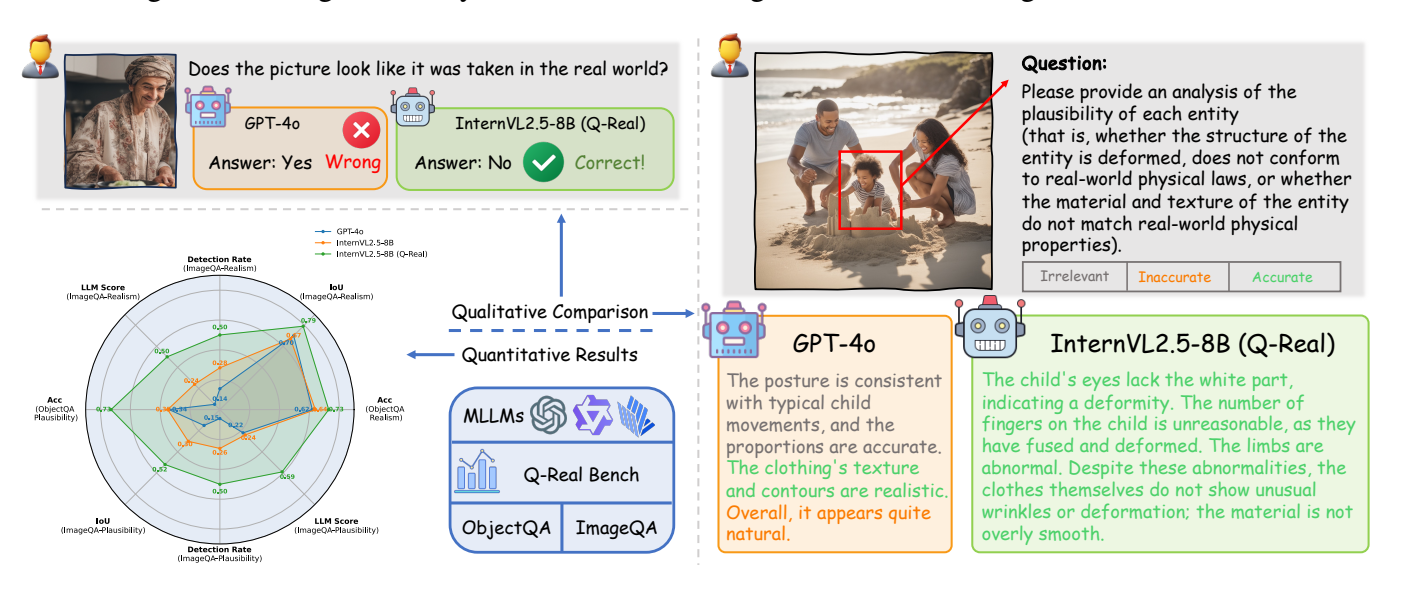


Figure 1. Abilities of Q-Real-tuned InternVL2.5-8B on two kinds of fine-grained quality assessment in AI-generated images, in comparison with the baseline version and GPT-4o.

Abstract

Quality assessment of AI-generated content is crucial for evaluating model capability and guiding model optimization. However, most existing quality assessment datasets and models provide only a single quality score, which is too coarse to offer targeted guidance for improving generative models. In current applications of AI-generated images, Realism and Plausibility are two critical dimensions, and with the emergence of unified generation—understanding models, fine-grained evaluation along these dimensions becomes especially effective for improving generative performance. Therefore, we introduce Q-Real, a novel dataset for fine-grained evaluation of realism and plausibility in AI-generated images. Q-Real consists of 3,088 images generated by popular text-to-image models. For each image, we annotate the locations of major entities and provide a set of judgment questions and attribution descriptions for these along the dimensions of realism and plausibility.

Considering that recent advances in multi-modal large language models (MLLMs) enable fine-grained evaluation of AI-generated images, we construct **Q-Real Bench** to evaluate them on two tasks: judgment and grounding with reasoning. Finally, to enhance MLLM capabilities, we design a fine-tuning framework and conduct experiments on multiple MLLMs using our dataset. Experimental results demonstrate the high quality and significance of our dataset and the comprehensiveness of the benchmark. Dataset and code will be released upon publication.

1. Introduction

With the rapid advancement of generative AI, massive amounts of text-to-image content are being produced and applied across various domains [13, 29]. However, some content is not always flawless and often require quality assessment before practical application. Moreover, the iterative improvement of generative models also relies on effective evaluation mechanisms to measure progress and guide

[†]Corresponding author.

optimization. Consequently, substantial efforts [14, 16, 37, 38] have been devoted to developing automated methods for assessing the quality of AI-generated content. However, existing datasets and models [33, 47] for evaluating AI-generated images often provide only a single quality score, resulting in vague and incomplete assessments. This fails to reveal issues and offer limited guidance for model improvement. Thus, fine-grained evaluations are essential for capturing image quality and advancing generative models.

Recent advances in Multi-modal Large Language Models (MLLMs) [2, 5, 18, 24] have shown strong capabilities in multi-modal tasks, offering opportunities for fine-grained evaluation. However, existing MLLMs are exposed to limited data on fine-grained quality assessment tasks during training, which making it difficult to learn deeper quality-related features and hinders their effectiveness in such evaluation scenarios [34, 36, 46, 48], as shown in Figure 1. Therefore, fine-grained evaluation datasets are needed to unlock the potential of MLLMs, enabling them to provide more informative assessment about AI-generated images.

To address these challenges, we introduce Q-Real, a novel fine-grained dataset for evaluating AI-generated images. The dataset comprises 3,088 images generated by 10 popular text-to-image (T2I) models, using 534 diverse prompts to ensure comprehensive content and styles. To enable more fine-grained quality assessment of AI-generated images, we annotated key objects in each image along two core dimensions: Realism and Plausibility. Realism measures whether an image appears visually natural and credible, while plausibility assesses whether the image content conforms to common sense. These two dimensions are the most relevant to users and downstream applications and serve as primary criteria for evaluating the performance of generative models. Using a novel automated annotation pipeline, we annotated the coordinates of key objects in each image with bounding boxes. For each object, we provided 2 judgment question-answer pairs and a reasoning description for realism, and 4 judgment question-answer pairs with a reasoning description for plausibility. Additionally, given the higher annotation difficulty and application importance of portrait images, we conducted fully manual annotations for 500 portrait images in our dataset. This design allows for a fine-grained, structured assessment of each AIgenerated image along both dimensions.

Based on this dataset, we construct the benchmark **Q-Real Bench**, as shown in Figure 2, which consists of two tasks: **ObjectQA** and **ImageQA**. In the ObjectQA task, models are required to answer judgment questions about the realism and plausibility of key objects in the image. In the ImageQA task, models are tasked with understanding the entire image, localizing objects that exhibit issues in realism or plausibility, and providing detailed descriptions of these issues. Specially, ObjectQA evaluates a model's basic

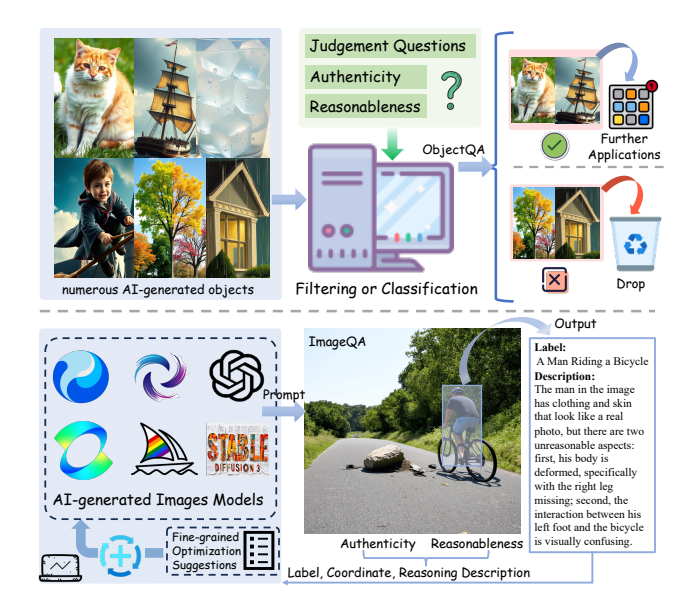


Figure 2. Application scenarios of ObjectQA and ImageQA in Q-Real Bench. ObjectQA can be used for large-scale image screening, while ImageQA provides fine-grained descriptions that can facilitate the optimization of generative models.

ability to judge the realism and plausibility of images, while ImageQA measures its overall understanding and analysis. Besides, ObjectQA is useful in practice for quickly filtering problematic entities in generated images, while ImageQA is valuable for real-world applications that require locating and explaining issues to provide better optimization signals for generative models.

To enhance the performance of MLLMs on Q-Real Bench, we propose a **Task-Specific Finetuning** framework. We construct two fine-tuning datasets aligned with the benchmark tasks: an ObjectQA dataset, consisting of object-level judgment QA pairs, and an ImageQA dataset, consisting of image-level grounding and reasoning description. Experimental results demonstrate that our method significantly improves the performance of MLLMs. Our main contributions are summarized as follows:

- We present Q-Real, the first fine-grained quality evaluation dataset for AI-generated images along the dimensions of Realism and Plausibility, constructed using an automated annotation pipeline.
- We design Q-Real Bench, comprising ObjectQA and ImageQA, to offer a comprehensive evaluation framework that systematically examines the capacity of MLLMs to judge both realism and plausibility in finegrained quality assessment.
- We propose a Task-Specific Finetuning framework and conduct experiments on multiple MLLMs, demonstrating the high quality of the dataset, the comprehensiveness of the benchmark, and the effectiveness of our approach in enhancing fine-grained evaluation.

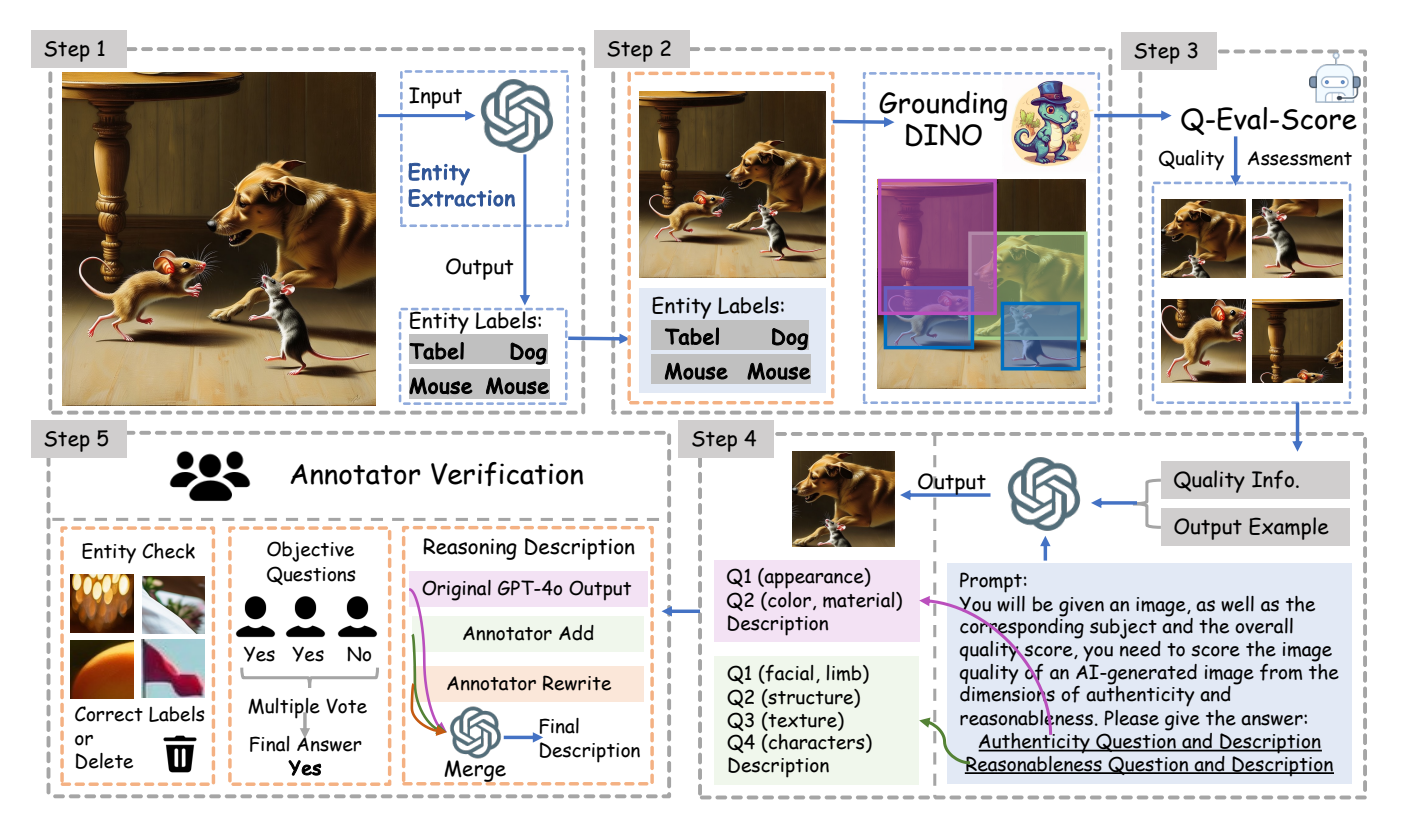


Figure 3. The pipeline of our dataset construction.

2. Related Work

2.1. AI-generated Image Quality Assessment

The evaluation of AI-generated images has become increasingly important as generative models like GAN [11], diffusion [12] and auto regressive models [31] continue to advance. Initially, metrics such as PSNR [27] and LPIPS [40] were used for these quality assessment. These metrics focused primarily on pixel-wise differences or perceptual feature similarities. This led to the creation of datasets such as AGIQA-3K [16], AIGIQA-20K [17] and Q-Eval-100K [47], which include mean opinion score (MOS) based annotations, as well as Pick-a-Pic [14] and HPS [37], where quality is annotated using the side-by-side (SBS) method. These datasets enabled models developed for usergenerated image quality assessment [15, 42, 45], such as LIQE [41], CLIP-IQA [32], and Q-Align [35], to also evaluate the quality of AI-generated images.

Although existing datasets and models have advanced AI-generated image quality evaluation, most still focus on overall quality and overlook local details. In the field of user-generated content quality assessment, some works such as Q-Instruct [36] and Grounding-IQA [7] have explored fine-grained evaluation strategies. For AI-generated images, RichHF [21] combines quality scores

with heatmaps to provide more detailed assessments of specific regions. In response to these developments, we propose Q-Real, which offers a more fine-grained quality assessment approach for AI-generated images by combining grounding with description-based evaluation of realism and plausibility, providing valuable feedback for AI-generated models optimization and refinement.

2.2. Multi-modality Large Language Models

Multi-modality Large Language Models (MLLMs) are models designed to process and understand multiple types of data such as text and images. These models bridge the gap between different modalities, enabling a unified understanding of both textual and visual information. Popular examples include LLaVA [18], InternVL [5], QwenVL [2] and GPT-40 [24], which excel at tasks such as visual question answering. With the rapid development of MLLMs, their applications have expanded to more complex multimodal scenarios, such as visual grounding [20, 26] and multimodal dialogue. With their cross-modal abilities, MLLMs have become foundational models for a wide range of visionand-language tasks [39]. However, current MLLMs often struggle with fine-grained quality assessment of AIgenerated images, particularly when it comes to evaluating nuanced details related to realism and plausibility [44]. To

address this limitation, we introduce Q-Real and finetune MLLMs on it, enabling more effective assessment of these two dimensions in AI-generated images.

3. Dataset

3.1. Q-Real Annotation Pipeline

A high-quality dataset is crucial for enabling models to perform fine-grained realism and plausibility evaluation. However, annotating such a dataset with subjective description is labor-intensive and costly. To address this challenge, we have developed a hybrid annotation strategy that combines automated annotation with manual verification, shown in Figure 3. The process is as follows:

- (1) Entity Name Extraction: Initially, we use GPT-40 [24] to extract the names of the entities appearing in the AI-generated images. Although extracting entity names directly from prompts may seem more straightforward, we instead adopt GPT-40 to analyze prompts and the images themselves, because AI-generated prompts often contain abstract or ambiguous descriptions that are not well aligned with the actual visual content. By directly processing the generated images, GPT-40 can identify the entities present more accurately and comprehensively, yielding better results than relying on text prompts alone.
- (2) Object Detection: For each extracted entity, we apply the Grounding DINO model [22] to detect the bounding box corresponding to the entity in the image. This allows precise localization of each object within the generated scene, enabling more accurate and comprehensive results compared to directly extracting all entities from the image using GPT-40 or other MLLMs.
- (3) Quality Evaluation: Following detection, we use the AI-generaetd image quality assessment model Q-Eval-Score [47] to assess the quality of each detected object. The quality score is crucial for generating analysis of realism and plausibility using GPT-40 or other MLLMs. While MLLMs excel at understanding image content, they still struggle with quality assessment. By incorporating quality scores, we provide GPT with a more grounded basis for evaluating the realism and plausibility of objects, ensuring that the generated descriptions better align with the true visual content of the image.
- (4) Generate Question-Answer Pairs and Reasoning Descriptions: Lastly, we input each extracted object along with its corresponding quality score into GPT-40. The model is then prompted to generate both objective judgment answers and reasoning descriptions regarding the extracted object's realism and plausibility. By incorporating quality scores, GPT-40 provides more accurate and reliable reasoning description. Through this automated annotation pipeline consisting of the first four steps, we obtain the initial version of the Q-Real dataset.



Figure 4. Detailed annotation protocol for Human Plausibility. Comparison between our fine-grained annotation and the conventional annotation approach for human regions.

(5) Manual Verification: After the automated annotation pipeline, a manual verification step is conducted to ensure annotation quality. Trained annotators review extracted objects and labels, filtering out those with small areas or poor clarity, and correcting any inconsistencies between image content and labels. For each object, three annotators verify both the objective judgment questions and the reasoning descriptions related to realism and plausibility. For judgment questions, each annotator answers independently, and the majority response is taken as final. For subjective descriptions, annotators supplement, revise or rewrite the GPT-40 generated content, and all inputs are combined to form the final evaluation. This process ensures the dataset's high quality and reliability for subsequent tasks.

3.2. Q-Real Dataset

To ensure the quality and diversity of our dataset, thereby enhancing the fine-grained quality evaluation capabilities of MLLMs, we adopt a wide range of advanced T2I generation models including Flux.1.dev [9], Stable Diffusion 3.0 [1], PixArt [4], Hunyuan-DiT [19], Kcolors [28], Dreamina [3], Midjourney [23], Lumina-T2X [10], WanX [8] and DALL·E 3 [25]. Meanwhile, prompts are designed to cover diverse entities (e.g., people, animals, objects) and visual attributes (e.g., color, texture, material), as well as varied physical interactions and contextual relevance.

With these models and prompt designs, we generate a total of 3,088 AI-generated images consisting of our dataset. After object detection, we extract entity regions from each image based on the predicted bounding boxes, yielding 17,879 entities for fine-grained evaluation of realism and plausibility. Each entity is further annotated with both objective and subjective assessments of its quality. Specifically, for each entity, two multiple-choice questions are

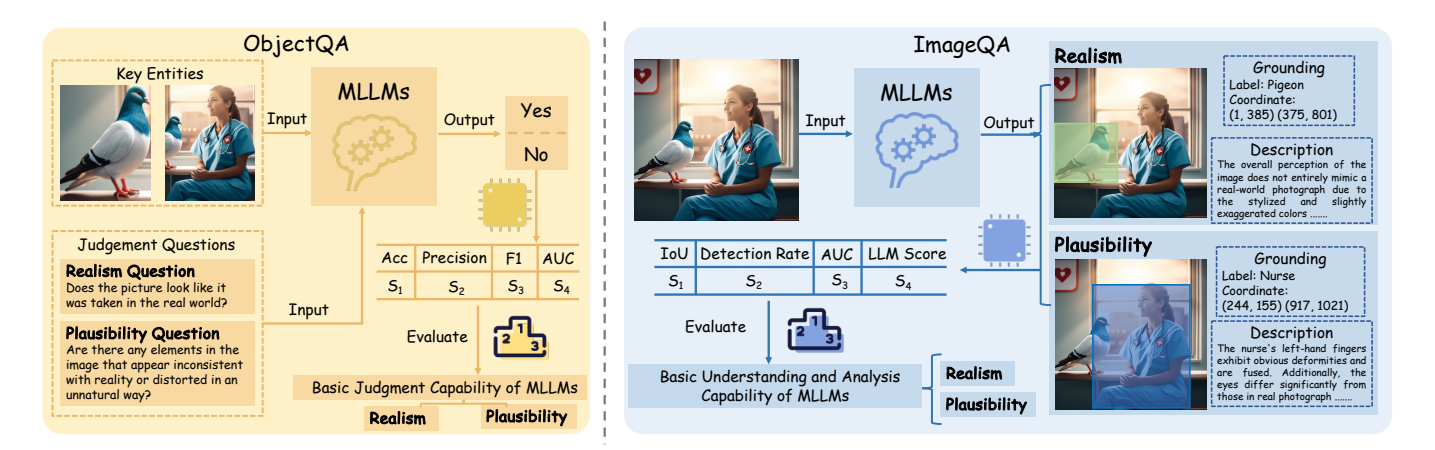


Figure 5. Overview of Q-Real Bench, illustrating its two tasks: ObjectQA and ImageQA, including evaluation procedures and metrics.

designed to evaluate the *realism* of the object, accompanied by a detailed rasoning description. Similarly, four multiple-choice questions are designed to assess the object's *plausibility*, along with an explanation. For each objective question and subjective description, three annotators are involved in the verification process to ensure annotation quality. In total, the dataset contains 17,879 x 8 x 3 = 429,096 high-quality annotations covering both realism and plausibility dimensions. Details of the judgment questions for assessing realism and plausibility, together with the reasoning descriptions for these two key dimensions, are presented below. For each detected entity, two judgment questions are constructed to evaluate its realism:

- 1. Does the picture look like it was taken in the real world?
- 2. Do the color, material texture, and lighting in the picture resemble those in the real world?

In addition, four judgment questions are formulated to assess the plausibility of these entities:

- 1. Does the facial or limb structure of the characters/animals/plants in the generated image appear abnormal or out of the ordinary?
- 2. Are there any elements in the image that appear inconsistent with reality or distorted in an unnatural way?
- 3. Does the material or texture of the objects in the image not match the real world?
- 4. Does the text within the image contain errors or garbled characters?

For the reasoning descriptions of these two key dimensions, the realism dimension focuses on specific visual attributes such as the object's color and material. It aims to identify the factors that cause the object to appear different from real images, highlighting discrepancies in visual realism. In contrast, the plausibility dimension concentrates on structural aspects, describing whether any parts of the object exhibit deformities, and whether the overall structure is different from the physical laws of the real world.

3.3. Fine-Grained Human Plausibility Annotation Protocol

For AI-generated models, creating human portraits is more challenging compared to other objects. This requires more detailed and accurate fine-grained quality descriptions as feedback to optimize the model's performance. To address this, we selected 400 human portrait images from Q-Real and performed additional fine-grained annotations on the plausibility dimension, shown in Figure 4. In detail, we required GPT-40 to provide reasoning descriptions for each human portrait across different dimensions. These include head/face, hands, limbs, torso, feet, clothing, and interactions with the surrounding environment. For each dimension, the descriptions were reviewed and supplemented by at least three annotators. Finally, the descriptions from all dimensions were integrated to form the overall reasoning description for the plausibility dimension.

3.4. Q-Real Bench

For evaluating model performance in Q-Real, we construct a benchmark, **Q-Real Bench**. The Q-Real Bench includes 400 images of various types and quality, which are selected from Q-Real Dataset. Based on this bench, we evaluate the performance of models in Q-Real from two perspectives: **ObjectQA** and **ImageQA**, as shown in Figure 5.

To evaluate the model's fundamental judgment ability about the realism and plausibility of AI-generated images, the task of **ObjectQA** requires the model to answer judgment questions regarding the two dimensions about selected key entities from Q-Real dataset. Since the ObjectQA task only requires the model to answer Yes or No, we adopt four standard metrics—Accuracy (*Acc*), *Precision*, *F1 Score*, and Area Under the ROC Curve (*AUC*) to comprehensively evaluate the performance of models in this task.

The task of **ImageQA** requires the model to perform fine-grained quality analysis on an AI-generated image, in-

cluding localizing the key entity with bounding boxes and providing reasoning descriptions regarding the realism and plausibility of each entity. Considering the most apparent distortion effect in quality assessment, we only assess the model's grounding and reasoning abilities on low quality regions, ensuring the evaluation targets the most challenging areas. This evaluation scheme provides a comprehensive reflection of whether MLLMs can effectively understand the realism and plausibility of AI-generated images.

To evaluate the model's grounding performance, we adopt two standard metrics: Intersection over Union (IoU), $Detection\ Rate$ and AUC. For computing IoU, we adopt the Hungarian matching algorithm to establish an optimal one-to-one correspondence between predicted and ground-truth entities. Specifically, given a set of predicted bounding boxes $\mathcal{P} = \{p_i\}_{i=1}^N$ and ground-truth boxes $\mathcal{G} = \{g_j\}_{j=1}^M$, we construct a cost matrix $C \in \mathbb{R}^{N \times M}$ based solely on coordinate overlap:

$$C_{ij} = 1 - \text{IoU}(p_i, g_j). \tag{1}$$

To obtain the optimal matching between predicted and ground-truth boxes, we solve this optimization problem:

$$\pi^* = \arg\min_{\pi} \sum_{i=1}^{K} C_{i\pi(i)}, \tag{2}$$

where π^* represents the optimal matching permutation, obtained by minimizing the objective function $\sum_{i=1}^K C_{i\pi(i)}$, with $C_{i\pi(i)}$ denoting the cost between the predicted and ground-truth boxes. Here, $K = \min(N, M)$ is the number of predicted and ground-truth boxes, where N is the number of predicted boxes and M is the number of ground-truth boxes. The final matched pairs are then used to compute the IoU. Detection Rate is defined as the fraction of predicted boxes that match a ground-truth box with an IoU threshold greater than 0.5. AUC here refers to the area under the curve of Detection Rate as a function of varying IoU thresholds, which reflects the overall detection performance across different localization strictness levels.

To evaluate the performance of models in reasoning description, we use the evaluation metric *LLM-Score*. The LLM-Score is calculated by inputting both the predicted description and the ground truth description into GPT-40 [30, 43], which then provides a semantic similarity score between the two texts. Compared to metrics such as BLEU@4 or cosine similarity of text embeddings, LLM-Score provides a more accurate evaluation of the semantic similarity between predicted and reference descriptions.

4. Task-Specific Finetuning for Fine-Grained Quality Assessment

Due to the limited ability of MLLMs to assess realism and plausibility in AI-generated images, directly training a

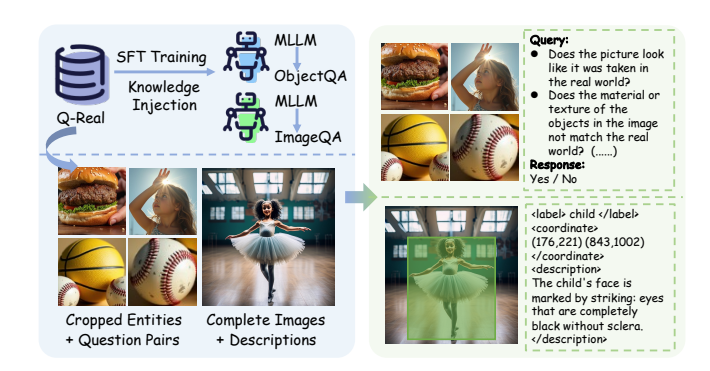


Figure 6. The data formats of different finetuning datasets constructed for ObjectQA and ImageQA tasks.

single model for fine-grained judgment, localization, and description is often ineffective. Therefore, we adopt a task-specific finetuning strategy for the two complementary tasks in Q-Real Bench and construct corresponding training datasets, as shown in Figure 6.

For **ObjectQA**, we finetune the MLLM using each key entity with its six question-answer pair about realism and plausibility from our dataset. Specifically, each training instance is formatted as two parts:

"query": "<image>Does the picture look like it was taken in the real world?"

"response": "No"

This training approach allows the model to concentrate on evaluating and analyzing the realism and plausibility of AI-generated entities, while minimizing interference from other irrelevant elements in the image.

For **ImageQA**, we construct a trainning dataset where each instance consists of a complete AI-generated image, the coordinates of entities (in the form of bounding boxes), and detailed reasoning descriptions, formatted as a comprehensive query-response pair. Due to the most apparent distortion effects, we include in the training set only the coordinates of entities with realism or plausibility issues along with their corresponding descriptions. This allows the model to learn more effectively and enhance its capability to distinguish problematic regions. Specifically, the format of training instance is structured as:

"query": <image> Analyze this AI-generated image, provide all entities with their type labels, coordinates within the image, and an explanation of plausibility (whether each entity looks like unnatural or not match the real world) for each object.

"response": "<label><coordinate><description> ... (repeated for each entity) "

By constructing task-specific datasets and individually finetuning MLLMs, we significantly enhance their ability to address the unique challenges of realism and plausibility evaluation in AI-generated images.

Table 1. Performance comparison of different models on the **ObjectQA** task. Evaluation metrics include $Acc \uparrow$, Precision \uparrow , F1 score \uparrow , and AUC \uparrow . The models marked with * indicate models fine-tuned using our proposed method. And *Realism Question 1*, Plausibility Question 1, etc., refer to the judgement questions in the realism and plausibility dimensions, as defined in Section 3.2.

| Model | Realism Question 1 | | | | Realism Question 2 | | | | Plausibility Question 1 | | | |
|---|--|---|---|---|---|---|---|--|--|--|--------------------------------------|-------------------|
| Wiodei | Acc | Precision | F1 Score | AUC | Acc | Precision | F1 Score | AUC | Acc | Precision | F1 Score | AUC |
| GPT-4o | 0.651 | 0.558 | 0.669 | - | 0.598 | 0.506 | 0.659 | - | 0.632 | 0.580 | 0.568 | - |
| Qwen2.5-VL-7B-Instruct | 0.665 | 0.677 | 0.432 | 0.761 | 0.650 | 0.609 | 0.465 | 0.710 | 0.578 | 0.709 | 0.087 | 0.681 |
| Qwen2.5-VL-7B-Instruct* | $0.729_{+6.4\%}$ | $0.677_{+0.0\%}$ | $0.649_{+21.7\%}$ | $0.800_{+3.9\%}$ | 0.726+7.6% | $0.671_{+6.2\%}$ | $0.653_{+18.8\%}$ | $0.797_{+8.7\%}$ | 0.786+20.8% | $0.732_{+2.3\%}$ | 0.764 _{+67.7%} | $0.870_{+18.9\%}$ |
| InternVL2.5-8B | 0.675 | 0.578 | 0.630 | 0.312 | 0.598 | 0.501 | 0.614 | 0.373 | 0.584 | 0.595 | 0.208 | 0.689 |
| InternVL2.5-8B* | $0.729_{+5.4\%}$ | $0.671_{+9.3\%}$ | $0.652_{+2.2\%}$ | $0.411_{+9.9\%}$ | 0.724+12.6% | 0.672+17.1% | $0.643_{+2.9\%}$ | $0.454_{+8.1\%}$ | 0.773+18.9% | 0.743+14.8% | 0.736 _{+52.8%} | $0.660_{-2.9\%}$ |
| llava-v1.6-mistral-7B | 0.636 | 0.541 | 0.577 | 0.679 | 0.539 | 0.462 | 0.606 | 0.641 | 0.605 | 0.547 | 0.521 | 0.661 |
| llava-v1.6-mistral-7B* | 0.737 _{+10.1%} | $0.692_{15.1\%}$ | $0.655_{+7.8\%}$ | $0.810_{+13.1\%}$ | $0.734_{+19.5\%}$ | $0.700_{+23.8\%}$ | $0.646_{+4.0\%}$ | $0.805_{+16.4\%}$ | 0.794 _{+18.9%} | $0.752_{+20.5\%}$ | 0.767 _{+24.6%} | $0.874_{+21.3\%}$ |
| | | | | | | | | | | | | |
| | 1 | Plausibility | Question 2 | | | Plausibility | Question 3 | | | Plausibility | Question 4 | |
| | Acc | Plausibility Precision | Question 2 F1 Score | AUC | Acc | Plausibility Precision | Question 3 F1 Score | AUC | Acc | Plausibility Precision | Question 4 F1 Score | AUC |
| GPT-40 | Acc 0.649 | | | AUC - | Acc 0.654 | | | AUC - | Acc 0.869 | | | |
| GPT-40 Qwen2.5-VL-7B-Instruct | | Precision | F1 Score | | | Precision | F1 Score | | | Precision | F1 Score | AUC |
| | 0.649 | Precision | F1 Score 0.756 0.369 | 0.648 | 0.654 | Precision - 0.722 - 0.853 | F1 Score 0.714 0.598 | | 0.869 | Precision 0.496 | F1 Score 0.616 0.106 | AUC |
| Qwen2.5-VL-7B-Instruct | 0.649 | Precision | F1 Score 0.756 0.369 | 0.648 | 0.654 | Precision - 0.722 - 0.853 | F1 Score 0.714 0.598 | | 0.869 | Precision - 0.496 - 0.700 | F1 Score 0.616 0.106 | AUC |
| Qwen2.5-VL-7B-Instruct Qwen2.5-VL-7B-Instruct* InternVL2.5-8B | 0.649 0.490 0.729 _{+23.9%} 0.610 | Precision 0.677 0.839 0.7429.7% 0.680 | F1 Score 0.756 0.369 0.805 _{+43.6%} 0.699 | 0.648 0.780 _{+13.2%} 0.561 | 0.654 0.629 0.714 _{+8.5%} 0.605 | Precision - 0.722 - 0.853 0.714 - 13.9% - 0.615 | F1 Score 0.714 0.598 0.787 _{+18.9%} 0.735 | 0.726 0.790 _{+7.0%} 0.448 | $ \begin{array}{r} -0.869 \\ -0.892 \\ 0.949_{\pm 5.7\%} \\ \hline 0.895 \end{array} $ | Precision - 0.496 - 0.700 0.811 +11.1% | F1 Score 0.616 0.106 0.758 0.245 | AUC |
| Qwen2.5-VL-7B-Instruct Qwen2.5-VL-7B-Instruct* InternVL2.5-8B | 0.649 0.490 0.729 _{+23.9%} 0.610 | Precision 0.677 0.839 0.7429.7% 0.680 | F1 Score 0.756 0.369 0.805 _{+43.6%} 0.699 | 0.648 0.780 _{+13.2%} 0.561 | 0.654 0.629 0.714 _{+8.5%} 0.605 | Precision - 0.722 - 0.853 0.714 - 13.9% - 0.615 | F1 Score 0.714 0.598 0.787 _{+18.9%} 0.735 | 0.726 0.790 _{+7.0%} 0.448 | $ \begin{array}{r} -0.869 \\ -0.892 \\ 0.949_{\pm 5.7\%} \\ \hline 0.895 \end{array} $ | Precision - 0.496 - 0.700 0.811 +11.1% - 0.638 | F1 Score 0.616 0.106 0.758 0.245 | AUC |

Table 2. Performance comparison of different models on the **ImageQA** task. Evaluation metrics include IoU \uparrow , Detection Rate (calculated with IoU threshold = 0.5) \uparrow , AUC \uparrow , and LLM Score \uparrow . The models marked with * indicate models fine-tuned using our proposed method.

| Model | Realism | | | | Plausibility | | | |
|-------------------------|------------------------|-------------------|-------------------|-------------------|--------------|-------------------|-------------------|-------------------|
| | IoU | Detection Rate | AUC | LLM Score | IoU | Detection Rate | AUC | LLM Score |
| GPT-4o | 0.141 | 0.054 | 0.153 | 0.343 | 0.146 | 0.056 | 0.153 | 0.219 |
| Qwen2.5-VL-7B-Instruct | 0.578 | 0.598 | 0.562 | 0.382 | 0.619 | 0.619 | 0.587 | 0.212 |
| Qwen2.5-VL-7B-Instruct* | 0.660 _{+8.2%} | $0.626_{+2.8\%}$ | $0.620_{+5.8\%}$ | $0.731_{+34.9\%}$ | 0.648+2.9% | $0.621_{+0.2\%}$ | $0.604_{+1.7\%}$ | $0.603_{+39.1\%}$ |
| InternVL2.5-8B | 0.283 | 0.241 | 0.279 | 0.355 | 0.304 | 0.256 | 0.298 | 0.245 |
| InternVL2.5-8B* | 0.498+21.5% | $0.503_{+26.2\%}$ | $0.454_{+17.5\%}$ | $0.732_{+38.7\%}$ | 0.518+21.4% | $0.503_{+24.7\%}$ | $0.456_{+15.8\%}$ | $0.588_{+34.3\%}$ |
| llava-v1.6-mistral-7B | 0.416 | 0.329 | 0.309 | 0.283 | 0.443 | 0.340 | 0.311 | 0.211 |
| llava-v1.6-mistral-7B* | 0.484 _{+6.8%} | $0.438_{+10.9\%}$ | $0.411_{+10.2\%}$ | $0.743_{+46.0\%}$ | 0.512+6.9% | $0.446_{+10.6\%}$ | $0.422_{+11.1\%}$ | $0.597_{+38.6\%}$ |

Table 3. Performance comparison of different models on the ImageQA task (The plausibility of human portrait images with finegrained annoation in the test set). The models marked with * indicate models fine-tuned using our proposed method.

| Model | IoU | Detection Rate | AUC | LLM Score |
|-------------------------|------------------------|-------------------|-------------------|-------------------|
| GPT-40 | 0.157 | 0.028 | 0.155 | 0.145 |
| Qwen2.5-VL-7B-Instruct | 0.716 | 0.736 | 0.691 | 0.155 |
| Qwen2.5-VL-7B-Instruct* | 0.717 _{+0.1%} | $0.653_{-8.3\%}$ | $0.639_{-5.2\%}$ | $0.504_{+34.9\%}$ |
| InternVL2.5-8B | 0.353 | 0.273 | 0.333 | 0.176 |
| InternVL2.5-8B* | $0.645_{+29.2\%}$ | $0.618_{+34.5\%}$ | $0.554_{+22.1\%}$ | $0.490_{+31.4\%}$ |
| llava-v1.6-mistral-7B | 0.618 | 0.442 | 0.388 | 0.127 |
| llava-v1.6-mistral-7B* | 0.632+1.4% | $0.596_{+15.4\%}$ | $0.535_{+14.7\%}$ | $0.479_{+35.2\%}$ |

5. Experiments

5.1. Experimental Settings

Implementation Details. We conduct experiments on four pre-trained multimodal models: Qwen2.5VL-7B [2], InternVL-8B [6], Ilava-v1.6-mistral-7B [18] and GPT-4o [24]. For the first three open-source MLLMs, we evaluate their performance both without finetuning and after finetuning on the training split of the Q-Real dataset using our task-specific finetuning framework, with all evaluations conducted on the Q-Real Bench. For GPT-4o, we only di-

rectly test its performance on this benchmark without any additional settings. This setup not only enables a comprehensive assessment of model capabilities in Q-Real Bench, but also demonstrates the effectiveness of our dataset in enhancing models' ability to reason about realism and plausibility in AI-generated content.

Training Settings. We fine-tune the models using LoRA with a cross-entropy loss. For ObjectQA training, we set the batch size to 4 and train for 3 epochs. For ImageQA training, the batch size is set to 2 with 5 training epochs. All other hyperparameters remain as the default settings of the base models. The experiments are conducted on 8 Nvidia A100-80G GPUs with Pytorch.

5.2. Findings on Q-Real Bench

The general performance on the ObjectQA and ImageQA tasks in Q-Real Bench is exhibited in Table 1 and Table 2, from which we can draw several conclusions:

1) For ObjectQA: Existing MLLMs initially demonstrate limited ability to judge realism and plausibility of AI-generated images, as Acc and F1 score are not both high, particularly when judging whether an object is real or distorted. After finetuning with Q-Real, both accuracy and F1

Table 4. Ablation study of task-specific finetuning in ImageQA. For each MLLM, ¹ and ² indicate training strategies 1 and 2, respectively, while * denotes our proposed optimal scheme. The best and second-best results for each metric are shown in **bold** and <u>underline</u>, respectively. Percentage change is calculated relative to our method.

| Model | | Reali | ism | | Plausibility | | | |
|-------------------------------------|------------------------|-------------------|-------------------|------------------|--------------|------------------|------------------|------------------|
| Wiodei | IoU | Detection Rate | AUC | LLM Score | IoU | Detection Rate | AUC | LLM Score |
| Qwen2.5-VL-7B-Instruct ¹ | 0.642 | 0.466 | 0.457 | 0.665 | 0.678 | 0.523 | 0.514 | 0.596 |
| Qwen2.5-VL-7B-Instruct ² | 0.653 | 0.519 | 0.513 | 0.738 | 0.634 | 0.538 | 0.534 | 0.606 |
| Qwen2.5-VL-7B-Instruct* | $0.660_{+0.7\%}$ | $0.626_{+10.7\%}$ | $0.620_{+10.7\%}$ | $0.731_{-0.7\%}$ | 0.648_3.0% | $0.621_{+8.3\%}$ | $0.604_{+7.0\%}$ | $0.603_{-0.3\%}$ |
| InternVL2.5-8B ¹ | 0.510 | 0.430 | 0.393 | 0.757 | 0.541 | 0.418 | 0.388 | 0.607 |
| InternVL2.5-8B ² | 0.488 | 0.471 | 0.434 | 0.731 | 0.503 | 0.479 | 0.440 | 0.577 |
| InternVL2.5-8B* | $0.498_{-1.2\%}$ | $0.503_{+3.2\%}$ | $0.454_{+2.0\%}$ | $0.732_{-2.5\%}$ | 0.518-2.3% | $0.503_{+2.4\%}$ | $0.456_{+1.6\%}$ | $0.608_{+0.1\%}$ |
| llava-v1.6-mistral-7B ¹ | 0.462 | 0.361 | 0.331 | 0.733 | 0.486 | 0.378 | 0.346 | 0.600 |
| llava-v1.6-mistral-7B ² | 0.420 | 0.370 | 0.346 | 0.737 | 0.445 | 0.381 | 0.345 | 0.597 |
| llava-v1.6-mistral-7B* | 0.484 _{+2.2%} | $0.438_{+6.8\%}$ | $0.411_{+6.5\%}$ | $0.743_{+0.6\%}$ | 0.512+2.6% | $0.446_{+6.5\%}$ | $0.422_{+7.6\%}$ | $0.597_{-0.3\%}$ |

score show clear improvements, with both metrics exceeding 0.7, which indicates enhanced understanding of realism and plausibility in AI-generated images.

2) For ImageQA: Existing MLLMs perform poorly on this task. For the grounding dimension, the detection of regions with realism and plausibility issues mainly depends on the model's inherent grounding capability. current MLLMs lack the ability to analyze the realism and plausibility of AI-generated images, and instead tend to output low-level visual flaws commonly seen in user-generated content. On fine-grained human plausibility annotations (shown in Table 3), their performance is even worse, with LLM Score dropping below 0.2. After finetuning, all MLLMs show notable improvements over their original performance, particularly in the description dimension. The LLM Score surpasses 0.7 for realism, whereas for plausibility it is close to 0.6. On the more challenging test set with fine-grained human plausibility annotations, the final score reaches 0.5, which is sufficient for practical use. Meanwhile, performance in the grounding dimension also improves, especially for models like InternVL2.5-8B, which originally had weaker grounding capabilities. For such models, both IoU and detection rate nearly double after finetuning.

These results on Q-Real Bench reveal the limitations of current MLLMs in analyzing the realism and plausibility of AI-generated images, while also demonstrating that our dataset and training framework can significantly improve their performance on these tasks.

5.3. Ablation Study

We conduct ablation experiments on ImageQA to demonstrate the effectiveness of our proposed Task-Specific Finetuning framework. We compare it with two alternative finetuning strategies, and the results are presented in Table 4. The two alternative strategies are as follows:

1) The ImageQA task is decomposed into three subtasks including entity detection, entity filtering, and reasoning description generating. Corresponding training datasets are constructed for each subtask, and models are fine-tuned separately. These models are then organized into an agent that

executes the subtasks sequentially to accomplish ImageQA.

2) A unified evaluation model is trained by first fine-tuning on a dataset constructed for ObjectQA, enabling the model to acquire fundamental judgment abilities regarding realism and plausibility. Building on this foundation, the model is further trained to perform ImageQA.

The experimental results demonstrate that the proposed Task-Specific Finetuning outperforms the two alternative methods in terms of average performance. In particular, it achieves a clear advantage on the grounding dimension while maintaining nearly the same level of accuracy in description generation. The superior performance of our method on the grounding dimension is mainly due to the framework's capacity to minimize error propagation across modules. In ImageQA, grounding requires the model to identify entities with issues in realism or plausibility. In contrast, both method 1 and method 2 split this into two separate subtasks-detection and judgment of problematic entities-leading to error accumulation between the modules, which adversely affects the final performance. Therefore, when finetuning MLLMs for complex tasks, choosing the most appropriate task decomposition strategy and constructing the corresponding training datasets is crucial to fully leverage the model and maximize final performance.

6. Conclusion

In conclusion, we propose Q-Real, the first fine-grained quality assessment dataset focusing on the realism and plausibility of AI-generated images. Building on this, we further design Q-Real Bench to systematically evaluate models' capabilities across multiple dimensions. Finally, we leverage Q-Real with our proposed training method to fine-tune several existing MLLMs. Experimental results show that Q-Real significantly enhances models' fine-grained understanding and analysis of AI-generated images, achieving strong performance on Q-Real Bench. We hope our work will inspire future research on advancing MLLMs for quality assessment of AI-generated content.

References

- [1] Stability AI. https://stability.ai. In Available through the Stability AI Developer Platform, 2023. 4
- [2] Shuai Bai, Keqin Chen, Xuejing Liu, Jialin Wang, Wenbin Ge, Sibo Song, Kai Dang, Peng Wang, Shijie Wang, Jun Tang, Humen Zhong, Yuanzhi Zhu, Mingkun Yang, Zhaohai Li, Jianqiang Wan, Pengfei Wang, Wei Ding, Zheren Fu, Yiheng Xu, Jiabo Ye, Xi Zhang, Tianbao Xie, Zesen Cheng, Hang Zhang, Zhibo Yang, Haiyang Xu, and Junyang Lin. Qwen2.5-vl technical report. In *arXiv preprint arXiv:2502.13923*, 2025. 2, 3, 7
- [3] Dreamina by CapCut. https://dreamina.capcut.com/. 2023.
- [4] Junsong Chen, Jincheng Yu, Chongjian Ge, Lewei Yao, Enze Xie, Yue Wu, Zhongdao Wang, James Kwok, Ping Luo, Huchuan Lu, et al. Pixart-α: Fast training of diffusion transformer for photorealistic text-to-image synthesis. In arXiv preprint arXiv:2310.00426, 2023. 4
- [5] Zhe Chen, Weiyun Wang, Yue Cao, Yangzhou Liu, Zhangwei Gao, Erfei Cui, Jinguo Zhu, Shenglong Ye, Hao Tian, Zhaoyang Liu, et al. Expanding performance boundaries of open-source multimodal models with model, data, and test-time scaling. In arXiv preprint arXiv:2412.05271, 2024. 2, 3
- [6] Zhe Chen, Jiannan Wu, Wenhai Wang, Weijie Su, Guo Chen, Sen Xing, Muyan Zhong, Qinglong Zhang, Xizhou Zhu, Lewei Lu, et al. Internvl: Scaling up vision foundation models and aligning for generic visual-linguistic tasks. In Proceedings of the IEEE/CVF Conference on Computer Vision and Pattern Recognition, 2024. 7
- [7] Zheng Chen, Xun Zhang, Wenbo Li, Renjing Pei, Fenglong Song, Xiongkuo Min, Xiaohong Liu, Xin Yuan, Yong Guo, and Yulun Zhang. Grounding-iqa: Multimodal language grounding model for image quality assessment. In *arXiv* preprint arXiv:2411.17237, 2024. 3
- [8] Alibaba Cloud. https://tongyi.aliyun.com/wanxiang/. 2024.
- [9] Black Forest Labs. Flux. https://github.com/black-forest-labs/flux. 2023. 4
- [10] Peng Gao, Le Zhuo, Chris Liu, Ruoyi Du, Xu Luo, Longtian Qiu, Yuhang Zhang, et al. Lumina-t2x: Transforming text into any modality, resolution, and duration via flow-based large diffusion transformers. In arXiv preprint arXiv:2405.05945, 2024. 4
- [11] Ian J. Goodfellow, Jean Pouget-Abadie, Mehdi Mirza, Bing Xu, David Warde-Farley, Sherjil Ozair, Aaron Courville, and Yoshua Bengio. Generative adversarial networks. In Advances in Neural Information Processing Systems, 2014. 3
- [12] Jonathan Ho, Ajay Jain, and Pieter Abbeel. Denoising diffusion probabilistic models. In *Advances in Neural Information Processing Systems*, 2020. 3
- [13] Everypixel Journal. Ai image statistics for 2024: How much content was created by ai. In *Everypixel*, 2024. 1
- [14] Yuval Kirstain, Adam Polyak, Uriel Singer, Shahbuland Matiana, Joe Penna, and Omer Levy. Pick-a-pic: An open dataset of user preferences for text-to-image generation. In

- Advances in Neural Information Processing Systems, 2020. 2, 3
- [15] Tengchuan Kou, Xiaohong Liu, Zicheng Zhang, Chunyi Li, Haoning Wu, Xiongkuo Min, Guangtao Zhai, and Ning Liu. Subjective-aligned dateset and metric for text-to-video quality assessment. In ACM International Conference on Multimedia, 2024. 3
- [16] Chunyi Li, Zicheng Zhang, Haoning Wu, Wei Sun, Xiongkuo Min, Xiaohong Liu, Guangtao Zhai, and Weisi Lin. Agiqa-3k: An open database for ai-generated image quality assessment. In *IEEE Transactions on Circuits and Systems for Video Technology*, 2023. 2, 3
- [17] Chunyi Li, Tengchuan Kou, Yixuan Gao, Yuqin Cao, Wei Sun, Zicheng Zhang, Yingjie Zhou, Zhichao Zhang, Weixia Zhang, Haoning Wu, et al. Aigiqa-20k: A large database for ai-generated image quality assessment. In *arXiv preprint* arXiv:2404.03407, 2024. 3
- [18] Feng Li, Renrui Zhang, Hao Zhang, Yuanhan Zhang, Bo Li, Wei Li, Zejun Ma, and Chunyuan Li. LLaVA-NeXT-Interleave: Tackling Multi-image, Video, and 3D in Large Multimodal Models. In arXiv preprint arXiv:2407.07895, 2024. 2, 3, 7
- [19] Zhimin Li, Jianwei Zhang, Qin Lin, Jiangfeng Xiong, Yanxin Long, Xinchi Deng, Yingfang Zhang, Xingchao Liu, Minbin Huang, Zedong Xiao, et al. Hunyuan-dit: A powerful multi-resolution diffusion transformer with fine-grained chinese understanding. In arXiv preprint arXiv:2405.08748.
- [20] Zhaowei Li, Qi Xu, Dong Zhang, Hang Song, Yiqing Cai, Qi Qi, Ran Zhou, Junting Pan, Li Zefeng, and Vu Tu. Groundinggpt: Language enhanced multi-modal grounding model. In Annual Meeting of the Association for Computational Linguistics, 2024. 3
- [21] Youwei Liang, Junfeng He, Gang Li, Peizhao Li, Arseniy Klimovskiy, Nicholas Carolan, Jiao Sun, Jordi Pont-Tuset, Sarah Young, Feng Yang, Junjie Ke, Krishnamurthy Dj Dvijotham, Katherine M. Collins, Yiwen Luo, Yang Li, Kai J Kohlhoff, Deepak Ramachandran, and Vidhya Naval-pakkam. Rich human feedback for text-to-image generation. In Proceedings of the IEEE/CVF Conference on Computer Vision and Pattern Recognition, 2024. 3
- [22] Shilong Liu, Zhaoyang Zeng, Tianhe Ren, Feng Li, Hao Zhang, Jie Yang, Chunyuan Li, Jianwei Yang, Hang Su, Jun Zhu, et al. Grounding dino: Marrying dino with grounded pre-training for open-set object detection. In arXiv preprint arXiv:2303.05499, 2023. 4
- [23] Midjourney. https://www.midjourney.com. 2023. 4
- [24] OpenAI. https://openai.com/index/gpt-4o. 2024. 2, 3, 4, 7
- [25] OpenAI and Dall·e 3. https://openai.com/dall-e-3. 2023. 4
- [26] Zhiliang Peng, Wenhui Wang, Li Dong, Yaru Hao, Shaohan Huang, Shuming Ma, and Furu Wei. Kosmos-2: Grounding multimodal large language models to the world. In *Interna*tional Conference on Learning Representations, 2024. 3
- [27] Gonzalez Rafael C and Paul Wintz. Digital image processing. In *Addison-Wesley Longman Publishing*, 1987. 3
- [28] Kolors Team. Kolors: Effective training of diffusion model for photorealistic text-to-image synthesis. In arXiv preprint, 2024. 4

- [29] Techreport. Ai image generator market statistics in 2024. In Techreport, 2024. 1
- [30] Aman Singh Thakur, Kartik Choudhary, and Venkat Srinik Ramayapally. Judging the judges: Evaluating alignment and vulnerabilities in Ilms-as-judges. In arXiv preprint arXiv:2406.12624, 2024. 6
- [31] Keyu Tian, Yi Jiang, Zehuan Yuan, Bingyue Peng, and Liwei Wang. Visual autoregressive modeling: Scalable image generation via next-scale prediction. In *arXiv* preprint *arXiv*:2404:02905, 2024. 3
- [32] Jianyi Wang, Kelvin CK Chan, and Chen Change Loy. Exploring clip for assessing the look and feel of images. In *AAAI Conference on Artificial Intelligence*, 2023. 3
- [33] Jiarui Wang, Huiyu Duan, Jing Liu, Shi Chen, Xiongkuo Min, and Guangtao Zhai. Aigciqa2023: A large-scale image quality assessment database for ai generated images: from the perspectives of quality, authenticity and correspondence. In CAAI International Conference on Artificial Intelligenc, 2023. 2
- [34] Haoning Wu, Zicheng Zhang, Erli Zhang, Chaofeng Chen, Liang Liao, Annan Wang, Chunyi Li, Wenxiu Sun, Qiong Yan, Guangtao Zhai, and Weisi Lin. Q-bench: A benchmark for general-purpose foundation models on low-level vision. In arXiv preprint arXiv:2309.14181, 2023.
- [35] Haoning Wu, Zicheng Zhang, Weixia Zhang, Chaofeng Chen, Chunyi Li, Liang Liao, Annan Wang, Erli Zhang, Wenxiu Sun, Qiong Yan, Xiongkuo Min, Guangtai Zhai, and Weisi Lin. Q-align: Teaching lmms for visual scoring via discrete text-defined levels. In arXiv preprint arXiv:2312.17090, 2023. 3
- [36] Haoning Wu, Zicheng Zhang, Erli Zhang, Chaofeng Chen, Liang Liao, Annan Wang, Kaixin Xu, Chunyi Li, Jingwen Hou, Guangtao Zhai, Geng Xue, Wenxiu Sun, Qiong Yan, and Weisi Lin. Q-instruct: Improving low-level visual abilities for multi-modality foundation models. In Proceedings of the IEEE/CVF Conference on Computer Vision and Pattern Recognition, 2024. 2, 3
- [37] Xiaoshi Wu, Yiming Hao, Keqiang Sun, Yixiong Chen, Feng Zhu, Rui Zhao, and Hongsheng Li. Human preference score v2: A solid benchmark for evaluating human preferences of text-to-image synthesis. In *arXiv preprint* arXiv:2306.09341, 2023. 2, 3
- [38] Jiazheng Xu, Xiao Liu, Yuchen Wu, Yuxuan Tong, Qinkai Li, Ming Ding, Jie Tang, and Yuxiao Dong. Imagereward: Learning and evaluating human preferences for texto-image generation. In *CoRR* 2304.05977, 2023. 2
- [39] Pan Zhang, Xiaoyi Dong, Bin Wang, Yuhang Cao, Chao Xu, Linke Ouyang, Zhiyuan Zhao, Haodong Duan, Songyang Zhang, and Shuangrui Ding. Internlmxcomposer: A visionlanguage large model for advanced text-image comprehension and composition. In arXiv preprint arXiv:2309.15112, 2023. 3
- [40] Richard Zhang, Phillip Isola, Alexei A. Efros, Eli Shechtman, and Oliver Wang. The unreasonable effectiveness of deep features as a perceptual metric. In *Proceedings of the IEEE Conference on Computer Vision and Pattern Recognition*, 2018. 3

- [41] Weixia Zhang, Guangtao Zhai, Ying Wei, Xiaokang Yang, and Kede Ma. Blind Image Quality Assessment via Vision-Language Correspondence: A Multitask Learning Perspective. In Proceedings of the IEEE/CVF Conference on Computer Vision and Pattern Recognition, 2023. 3
- [42] Zicheng Zhang, Chunyi Li, Wei Sun, Xiaohong Liu, Xiongkuo Min, and Guangtao Zhai. A perceptual quality assessment exploration for aigc images. In *IEEE International* Conference on Multimedia and Expo Workshops, 2023. 3
- [43] Zicheng Zhang, Ziheng Jia, Haoning Wu, Chunyi Li, Zijian Chen, Yingjie Zhou, Wei Sun, Xiaohong Liu, Xiongkuo Min, Weisi Lin, and Guangtao Zhai. Q-bench-video: Benchmarking the video quality understanding of lmms. In arXiv preprint arXiv:2409.20063, 2024. 6
- [44] Zicheng Zhang, Haoning Wu, Chunyi Li, Yingjie Zhou, Wei Sun, Xiongkuo Min, Zijian Chen, Xiaohong Liu, Weisi Lin, and Guangtao Zhai. A-bench: Are lmms masters at evaluating ai-generated images? In *arXiv preprint arXiv:2406.03070*, 2024. 3
- [45] Zicheng Zhang, Yingjie Zhou, Chunyi Li, Baixuan Zhao, Xiaohong Liu, and Guangtao Zhai. Quality assessment in the era of large models: A survey. In *arXiv preprint* arXiv:2409.00031, 2024. 3
- [46] Zicheng Zhang, Yingjie Zhou, Chunyi Li, Baixuan Zhao, Xiaohong Liu, and Guangtao Zhai. Quality assessment 842 in the era of large models: A survey. In *arXiv preprint* arXiv:2409.00031, 2024. 2
- [47] Zicheng Zhang, Tengchuan Kou, Shushi Wang, Chunyi Li, Wei Sun, Wei Wang, Xiaoyu Li, Zongyu Wang, Xuezhi Cao, Xiongkuo Min, Xiaohong Liu, and Guangtao Zhai. Q-eval-100k: Evaluating visual quality and alignment level for textto-vision content. In arXiv preprint arXiv:2503.02357, 2025. 2, 3, 4
- [48] Deyao Zhu, Jun Chen, Xiaoqian Shen, Xiang Li, and Mohamed Elhoseiny. Minigpt-4: Enhancing vision-language understanding with advanced large language models. In arXiv preprint arXiv:2304.10592, 2023. 2